Identification of Rotordynamic Parameters on a Test Stand with Active Magnetic Bearings

N.G. WAGNER; W.D. PIETRUSZKA

Mannesmann Demag, and University-GH-Duisburg
Duisburg, Germany

Summary

A rotor test stand using active magnetic bearings and a digital control unit to identify system parameters is presented. On the basis of a discrete-time system description, reference is made to a basic control circuit and a feasible identification method for on-line processing. First experimental results in terms of basic control circuit design and identification are discussed.

1. Introduction

Because of their physical properties and design, active magnetic bearings can perform further functions beyond that of supporting the shaft. Techniques of active vibration control [6, 7] and identifying parameters can be used particularly in conjunction with a digital control system. The identification of rotor-dynamic parameters in a test stand utilising active magnetic bearings allows to improve the reliability of rotor-dynamic calculations.

This is of major importance for turbo-compressor rotors as the trend towards ever increasing power density leads to the design of very slender rotors which are run far above their first natural bending frequency. Only with sufficiently precise knowledge of the bearing characteristics and the magnitude of the various excitation sources can stable operation be ensured through an adequate rotor-dynamic design [4, 5]. This applies to machines both with conventional bearings and with magnetic bearings.

The prediction of excitation by fluid forces originating from the inter-stage and shaft seals require results from experiments [3]. Realistic experiments can be conducted on a test

stand with active magnetic bearings serving as measuring unit. The objective of this paper is to present a rotor test stand for that purpose and a possible method of parameter identification.

The approach to be shown can be generalised and transferred to other rotor systems. On the one hand, it enables the controller parameters to be adapted with varying operating conditions such that an optimum rotor behaviour can always be achieved, and on the other it allows to match magnetic bearing units to unknown rotor systems at the start-up phase.

2. Test Stand

The use of active magnetic bearings allows flow tests under realistic conditions which prevail in this stand in contrast with conventional test stands, in particular:

a) Magnetic bearings may be installed in the pressure chamber. This allows tests at a *high pressure level* without shaft seals which would affect the dynamics of the entire system. Apart from the known magnetic forces and fluid forces, there are no further disturbing forces acting on the rotor if the shaft is well balanced.

b) Owing to the possibility of presetting test functions, magnetic bearings allow the simulation of a great variety of *real operating conditions*.

The test set-up employed is shown schematically in figure 1. In view of the algorithms to be processed a digital signal processing unit was developed because of the greater flexibility it offers. The core is a 16 bit signal processor with an on-board multiplier [7]. The assembler programs are set up in a host computer. The evaluation module (EVM) provides the connection between the host computer and the signal processor

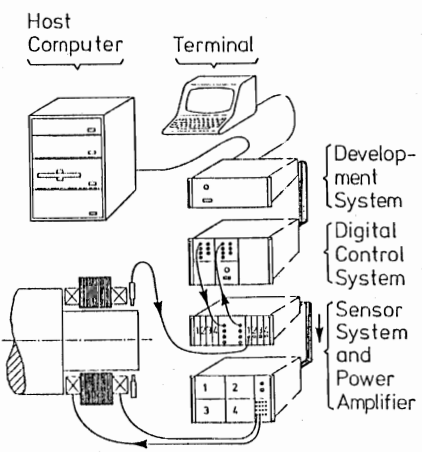

Fig. 1: Digital Signal Processing

and includes, inter alia, the assembler and debug options. The EVM processor and the signal processor work in a master/slave configuration. An analog interface with 7 input/output channels was developed at the Duisburg University as input/output of the signal processor [7]. Inductive sensors are used to measure distances and the power amplifiers are pulsed DC types.

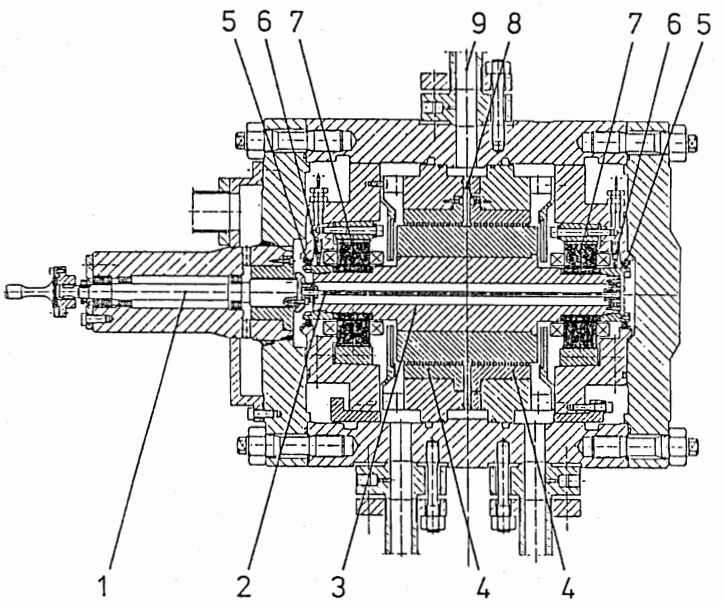

Fig. 2: Test stand with active magnetic bearings

Figure 2 is a sectional view of the test stand. The drive is conventional by a variable-speed motor via a gear unit. Since the drive is not integral with the stand, disturbing moments originating from the drive are avoided and the test rotor is simple and symmetric. The dynamic separation of the test rotor (3) from the drive (1) is through a most bendable and torsionally elastic bar (2) introduced through the hollow rotor. The figure shows a labyrinth seal being tested. The symmetric arrangement of two identical labyrinths (4) provides balanced thrust. The test gas is admitted in the casing centre (9) and accelerated tangentially by swirl rings (8). The magnetic bear-

ings (7) are jointly installed with the auxiliary bearings (5) and sensors (6) in a housing and are radially adjustable. The electrical lines to the sensors and bearings leave the housing through pre-stressed glass penetrations.

3. Equations of Motion

The test shaft shown in figure 2 is projected to the model of the rigid rotor according to figure 3. The axial motion need not be considered because of being restrained by the torsion bar. The radial rotor motions are described by the coordinates of centre of gravity x, y, and cardan angles α, β. Magnetic forces F_r and F_l act in the right and in the left bearing plane. The flexural stiffness of the torsion bar is simulated by a substitute spring with stiffness factor k_a at the right shaft end. Furthermore a static unbalance $F = m\ e\ \Omega^2\ \exp(j\Omega t)$ and a dynamic unbalance

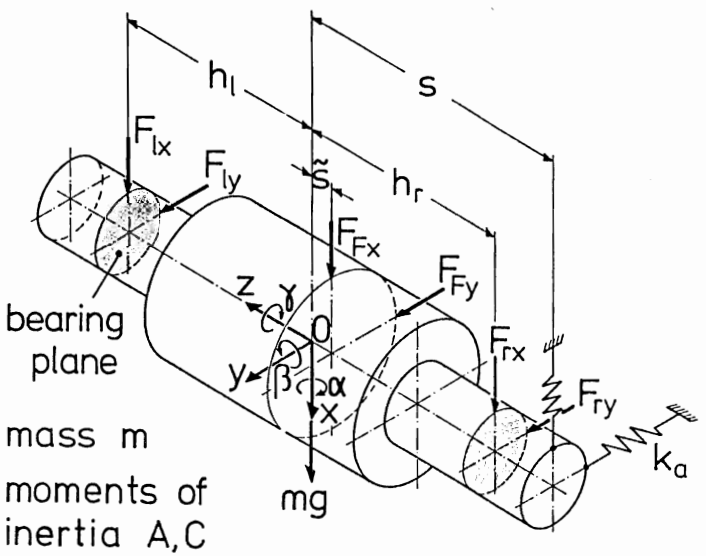

Fig.3: Model of rigid rotor, coordinate system

$M = E\,\Omega^2 \exp(j\Omega t)$ has to be considered ($j = \sqrt{-1}$). The resulting fluid forces ideally act at the rotor centre where because of inevitable unsymmetry, axial shift $\tilde{s}$ of that force has to be considered. In the event of little vibration x, y of the rotor about the centre these fluid forces can be taken as proportional to deflection and velocity [3], with coefficients d_R, d_Q, k_R, k_Q which are unknown at this stage:

$$\begin{bmatrix} F_{Fx} \\ F_{Fy} \end{bmatrix} = -\begin{bmatrix} d_R & d_Q \\ -d_Q & d_R \end{bmatrix}\begin{bmatrix} \dot{x} \\ \dot{y} \end{bmatrix} - \begin{bmatrix} k_R & k_Q \\ -k_Q & k_R \end{bmatrix}\begin{bmatrix} x \\ y \end{bmatrix} \qquad (1)$$

The angles α, β of rotor incline are not considered in equation (1) since disturbing moments which may occur are compensated, which results in the rotor performing pure motions of translation.

In the case of minor motions about the centre the magnetic forces for the left and the right bearing (index l, r) can be linearised [2, 8, 9]. Therefore the bearing force can be expressed as

$$\begin{bmatrix} F_x \\ F_y \end{bmatrix}_{l,r} = k_s \begin{bmatrix} x_L \\ y_L \end{bmatrix}_{l,r} + k_q \begin{bmatrix} i_x \\ i_y \end{bmatrix}_{l,r} \qquad (2)$$

where x_L, y_L bearing coordinates; i_x, i_y bearing currents, and $k_s = \mu_o N^2 A_L I_o^2/s_o^3$, $k_q = 0{,}5\,\mu_o N^2 A_L I_o/s_o^2$ with $\mu_o = 4\pi\ 10^{-7}$ Vs/Am, N number of windings; A_L pole surface; I_o magnetic biasing current; s_o nominal air gap.

Employing the complex variables $z = x + j\,y$ and $\varphi = \beta - j\,\alpha$ and the complex bearing currents in the left and the right bearing $u_l = i_{lx} + j\,i_{ly}$, $u_r = i_{rx} + j\,i_{ry}$, the linear motion equations, taking account of the gyroscopic influence, can be expressed as:

$$\begin{bmatrix} m & 0 \\ 0 & A \end{bmatrix}\begin{bmatrix} \ddot{z} \\ \ddot{\varphi} \end{bmatrix} + \begin{bmatrix} D_{11} & 0 \\ \tilde{s}\,D_{11} & D_{22} \end{bmatrix}\begin{bmatrix} \dot{z} \\ \dot{\varphi} \end{bmatrix} + \begin{bmatrix} C_{11} & C_{12} \\ C_{21} & C_{22} \end{bmatrix}\begin{bmatrix} z \\ \varphi \end{bmatrix} =$$

$$= \begin{bmatrix} me \\ E \end{bmatrix}\Omega^2 \exp(j\Omega t) + k_q \begin{bmatrix} 1 & 1 \\ h_l & -h_r \end{bmatrix}\begin{bmatrix} u_l \\ u_r \end{bmatrix} + \begin{bmatrix} mg \\ 0 \end{bmatrix} \qquad (3)$$

with the following expressions (cf. Fig. 3):

$$D_{11} = 2(d_R - jd_Q) \qquad C_{12} = -k_a s - k_s(h_l - h_r)$$

$$D_{22} = -j\Omega C \qquad C_{21} = -k_a s - k_s(h_l - h_r) + 2k_R\tilde{s} - j2k_Q\tilde{s}$$

$$C_{11} = k_a + 2(k_R - k_s) - j2k_Q \qquad C_{22} = k_a s^2 - k_s(h_r^2 - h_l^2)$$

Generally, motions of the centre of gravity and incline z,φ occur as combined motions. In the present case (cf. Fig. 2) the two bearings are at the same distance from the centre of gravity, i.e. $h_l = h_r$. The equations can be completely separated if the fluid forces act exactly at the rotor centre($\tilde{s} = 0$) and the flexural stiffness of the torsion bar is negligible ($k_a = 0$). We shall use these simplifications in our further approach.

Owing to the digital signal processing method we use, the system works on the sampling principle with the result that the analysis is continued in a discrete-time manner. The conversion of the continuous-time representation (3) into the discrete-time representation is accomplished using the transition matrix [1]. For the complex motion of centre of gravity we employ a derived difference equation which only contains the deflections involved:

$$z(k) + a_1 z(k-1) + a_2 z(k-2) = b_1 u(k-1) + b_2 u(k-2) + w_G + w_o + w_s s(k-1) \quad (4)$$

with the complex system parameters a_1, a_2, b_1, b_2, into which enter, inter alia, the fluid forces, with the control variable $u(k) = u_l(k) + u_r(k)$, variable of unbalance w_s (time function: $s(k-1) = \exp(j\Omega(k-1)T)$)as well as weight w_G and an additional constant disturbance w_o. If we now introduce backward shift operator q^{-1}, equation (4)can be transformed into

$$\left[1 + A(q^{-1})\right] z(k) = B(q^{-1})u(k) + w_G + w_o + w_s s(k-1) \quad (5)$$

using the polynomials

$$A(q^{-1}) = a_1 q^{-1} + a_2 q^{-2}; \quad B(q^{-1}) = b_1 q^{-1} + b_2 q^{-2}$$

4. Basic Control Circuit

If the fluid forces are not considered now, the known parameters in $A_o(q^{-1})$, $B_o(q^{-1})$ can be used, with $\Omega = \Omega_A$ as given design angular velocity, to present the control law

$$u_o(k) = -\frac{1}{P(q^{-1})}\left[Q(q^{-1})z(k)+u_G\right] \qquad (6)$$

for the system free of unbalance

$$\left[1+A_o(q^{-1})\right] z(k) = B_o(q^{-1})u_o(k)+w_G \qquad (7)$$

In equation (6) P and Q stand for polynomials

$$P(q^{-1}) = 1+p_1\, q^{-1}; \qquad Q(q^{-1}) = q_o+q_1\, q^{-1} \qquad (8)$$

with initially unknown coefficients for matching to the rotor dynamics desired. The compensation of weight is by means of u_G.

In the simplest case the controller coefficients in (6) are determined by placing poles z_i (i=1,2,3) for the control circuit taken from (6) and (7). This leads to coefficient comparison [1] of the form

$$P(z^{-1})\left[1+A_o(z^{-1})\right] + B_o(z^{-1})\, Q(z^{-1}) = \prod_{i=1}^{3}(z-z_i) \qquad (9)$$

with single-valued coefficients for the basic control circuit.

5. Identification of Parameters

Figure 4 is a typical representation of the parameter identification procedure.

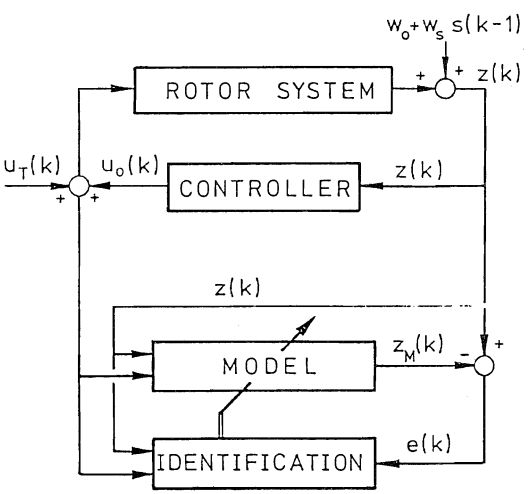

Fig. 4:
Typical procedure of parameter identification

This diagram shows the rotor system with parameter vector

$$\underline{p}^T = \left[a_1, a_2, b_1, b_2, w_o, w_s\right] \qquad (10)$$

connected in parallel with an equally structured deterministic model including external disturbance with adjustable parameters

$$\underline{p}_M^T(k) = \left[a_{M1}(k), a_{M2}(k), b_{M1}(k), b_{M2}(k), w_{Mo}(k), w_{Ms}(k) \right] \tag{11}$$

Error

$$e(k) = z(k) - z_M(k) = \left[\underline{p} - \underline{p}_M(k) \right]^T \underline{\Phi}(k-1) = \underline{\Delta p}^T(k)\, \underline{\Phi}(k-1) \tag{12}$$

with data vector

$$\underline{\Phi}^T(k-1) = \left[-z(k-1), -z(k-2);\ u(k-1), u(k-2);\ 1;\ s(k-1) \right] \tag{13}$$

tends towards zero if

$$\underline{p}_M(k) \longrightarrow \underline{p} \qquad \text{for } k \longrightarrow \infty$$

In contrast with (6), the variable in (13) is to be extended by the test signal $u_T(k)$:

$$u(k) = u_o(k) + u_T(k).$$

On the basis of error (12) there are numerous methods which can be employed to draft a suitable on-line identification algorithm. Since the hardware and numeric expenditure must be within reasonable limits, currently two approaches can be highlighted: one is the well-proved least squares method which is most advantageous in that it provides rapid convergence with well selected initial values. However, its disadvantage is the still high numeric expenditure for quick on-line identification. On the other hand, the minimisation of e(k) using the gradient method has proved to be successful. This approach ist characterised by a low numeric expenditure. Its disadvantage is the slow convergence and the related greater susceptibility to disturbance. Despite these disadvantages we are using the gradient method for error minimisation.

Taking the real error function

$$J(\underline{p}_M(k)) = \frac{1}{2}\, e(k)\, \bar{e}(k) \tag{14}$$

$$= \frac{1}{2}\, \underline{\Phi}^T(k-1)\, \underline{\Delta p}(k)\, \overline{\underline{\Delta p}}^T(k)\, \bar{\underline{\Phi}}(k-1),$$

in which the superlined values represent the conjugate complex numbers, and the related gradient

$$\operatorname{grad}(J(\underline{p}_M(k)) = \bar{\underline{\Phi}}(k-1)\, e(k) \tag{15}$$

as a basis, we obtain the identification algorithm

$$\underline{p}_M(k+1) = \underline{p}_M(k) + \underline{G}(k)\ \overline{\underline{\Phi}}(k-1)\ e(k). \tag{16}$$

For the hermitic weighting matrix $\underline{G}(k) = \overline{\underline{G}}^T(k)$ we write:

$$\underline{G}(k) = \frac{c_0}{\overline{\underline{\Phi}}^T(k-1)\ \underline{G}_0\ \underline{\Phi}(k-1)}\ \underline{G}_0 \qquad 0 < c_0 < 2 \tag{17}$$

with the constant diagonal matrix $\underline{G}_0$.

If the system-parameters are known, the disturbances can be identified separately.

Figure 5 gives an exemplary result of a numeric simulation of error e(k) and identification variable $a_{M1}(k)$ varying as a function of time. We see the error initially decreasing relatively fast. As mentioned above, the residual adaptive variation of $a_{M1}(k)$ is slow because of the small residual error. This behaviour causes some difficulties during processing with the aid of a micro computer and requires the selection of suitable scales.

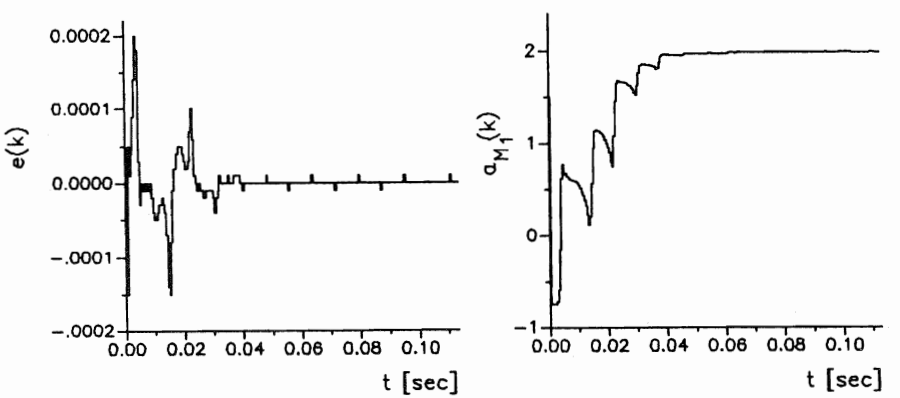

Fig. 5: Numeric simulation of the identification process

6. Experimental Results

At first we are discussing the behaviour of the basic control circuit. The problem faced when designing a digital control circuit is to correctly tune the controller coefficients and the sampling time with due consideration of the permanent disturbance of the measuring signal by noise. Most of this fine adjustment cannot be accomplished but by way of experiment. The test rotor showed a favourable running behaviour with 500 µs sampling time and poles placed between z_i = 0.70 ... 0.85 (i=1,...,6). However, here the static stiffness is low resulting in the weight having to be compensated by constant superimposition of u_G in (6) or the static stiffness being increased through an integrating portion.

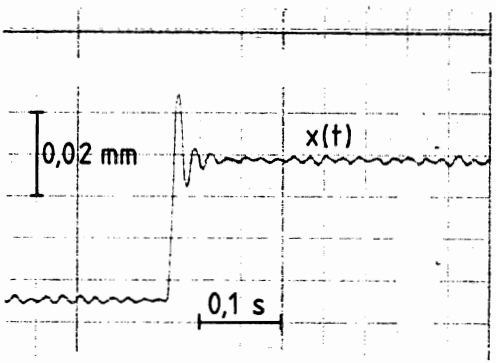

Fig. 6: Step response. Sampling time T=500 µs

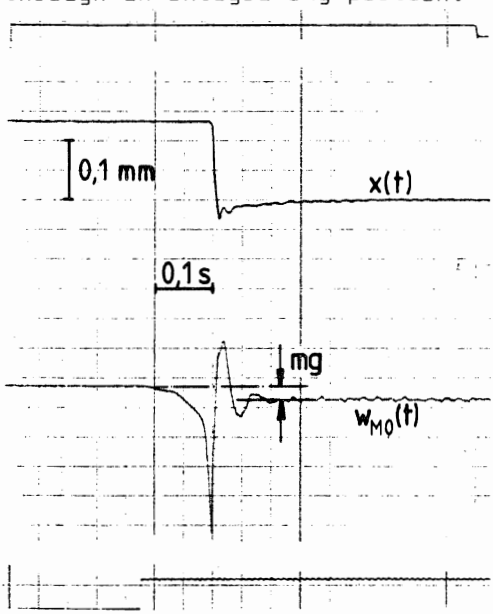

Fig. 7: Parameter identification

Figure 6 shows the deflection of centre of gravity x(t) when a reference signal is changed abruptly, the weight being compensated by u_G in (6) instead of an integrating portion. We readily see a good settling time to the new final condition. The identification algorithm is to be judged in the first analysis on the basis of the determination of the weight parameter w_0 in (4) and (10). Figure 7 is based on the system with the basic control circuit according to (6) (u_G=0) and shows the identification process as a function of time giving deflection signal x(t) and parameter $w_{M0}(t)$. The identification process is completed after 0.2 seconds, and the identification time and the signal overshoot can be influenced by selecting a different weighting coefficient c_0 in (17).

References

/1/ Ackermann, J.: Abtastregelung, Springer, Berlin, 1983

/2/ Bleuler, H.: Decentralized Control for Magnetic Rotor Bearing Systems, Diss. ETH Zürich, 1984

/3/ Childs, D., Scharrer, J.: Experimental Rotor Dynamic Coefficient Results for Teeth-on-rotor and Teeth-on-stator Labyrinth Gas Seals, ASME-Paper 86-GT-12, Gas Turbine Conference and Exhibition, Düsseldorf, 1986

/4/ Fulton, J.W.: The Decision to Full Load Test a High Pressure Centrifugal Compressor in its Module Prior to Tow-out, Inst.Mech.Eng. Conf.Publ. 1984-2, The Hague, March 1984

/5/ Wang Xi-Xuan, Gu Jin-chu, Shen Qin-gen, Huan Yong Li, Zhu Lan-sheng: Some Field Experiences with Subsynchronous Vibration in Centrifugal Compressors, Proceedings of the Fifth Workshop on Rotordynamic Instability Problems in High-performance Turbomachinery, Texas A & M University, College Station, Texas, May 16-18, 1988

/6/ Pietruszka, W.D., Wagner, N.: Aktive Beeinflussung des Schwingungsverhaltens eines magnetisch gelagerten Rotors, VDI-Berichte Nr. 456, 1982

/7/ Pietruszka, W.D.: Zeitdiskrete Schwingungsbeeinflussung magnetisch gelagerter Rotoren mit Mikrorechnern, VDI-Berichte Nr. 603, 1986

/8/ Traxler, A.: Eigenschaften und Auslegung von berührungsfreien elektromagnetischen Lagern, Diss. ETH Zürich, 1985

/9/ Ulbrich, H.: Entwurf und Realisierung einer berührungsfreien Magnetlagerung für ein Rotorsystem, Diss. TU München, 1979

Unbalance and Disturbance Control